

Micro Structural and Optical Properties of Ferrous Selenide Thin Films and Its Characterization

Segu Sahuban Bathusha NM¹, Chandra Mohan R^{2*}, Saravana Kumar. S², Ayeshamariam A^{3*} and Jayachandran M²

¹Department of Physics, Syed Hameedha Arts and Science College, Kilakarai-623 517, India

²Department of Physics, Sree Sevugan Annamalai College, Devakottai, 630303, India

³Department of Physics, Khadir Mohideen College, Adirampattinam, 614701, India

Abstract

Ferrous Selenide (FeSe) thin films were prepared onto glass substrate by Electron beam evaporation technique. X-Ray Diffractometer analyses showed that highly c-axis oriented and high-quality films were obtained on various annealing temperatures of 100°C, 200°C and 300°C respectively. From Scanning Electron Microscopy and its Elemental analysis of all the films showed low-temperature structural phase transition at different annealing temperatures of RT, 100°C, 200°C and 300°C respectively. The optical studies of FeSe thin film on glass was found most different from all the others, and its bandgap decreases from 2.85 eV to 2.75 eV for different annealing temperatures of the thin films. Optical analysis is demonstrated that Ferrous (Fe) and Selenide (Se) are homogeneously distributed in the film. Atomic Force Microscopy (AFM) and its 2D and 3D analyses were found that microstructure of FeSe thin films.

Keywords: Optical; Morphology; Structural and FeSe thin films

Introduction

The expansion of nano-science and nanotechnology rely heavily on the preparation techniques and associated study of nano scale materials of enhanced characteristics and their functionalities that forms nanostructure for novel modern devices. Dual semiconductors are considered to be significant technological materials their impending applications in opto-electronic devices, solar cells, Infra-Red (IR) detectors and lasers [1-5].

A multitude of techniques like thermal evaporation, sputtering, chemical deposition, electrolysis, spray pyrolysis and other have been developed to prepare thin films. In the early stages, the behavior of thin films, irreproducible results had often initiated the scientific curiosity towards thin film studies. In the last three decades there have been tremendous advances in understanding the properties of two dimensional solids. Thin film studies have indirectly advanced many areas of research based on phenomenon uniquely characteristic of the thickness, geometry and structure of the films.

It is well known that the semiconducting materials particularly semiconducting thin films have significant physical and chemical properties which are often sharply improved by combining them in different properties for their alloys (or) compounds. The use of both amorphous and polycrystalline semiconductors has attracted much interest in an expanding variety of applications in various electronic and optoelectronic devices.

The study of X-ray diffraction patterns revealing the position broadening and shape variation of X-ray profiles on the polycrystalline thin film offers information about the microstructural parameters which differentiates the microstructural dissimilarities in the thin nano and micro films of FeSe. Particle size, strain, dislocation density manipulate the properties of e-beam evaporation deposited thin films.

In addition, the stress, dislocation density and enlarge grain sizes of FeSe films possibly functional for opto-electronic appliances. To great extent attention among II-VI group compounds has been given to iron chalcogenides, for the reason that of their potential absorber in solar cells and other electrical devices. FeSe has a direct band gap of 1.23 eV which makes it quite attractive for solar cells. For the polycrystalline FeSe thin film that are habitually crystallized primarily in tetragonal

structure (PDF-03-0533) with lattice constants ($a=3.77^\circ\text{\AA}$, $c=5.53^\circ\text{\AA}$) and in the hexagonal structure (PDF-75-0608) with lattice constants ($a=3.61^\circ\text{\AA}$, $c=5.87^\circ\text{\AA}$). A wide range of procedures have been accounted for the preparation of FeSe semiconductor to get hold of appliance quality of thin films. Several case in points are as: low pressure metal organic chemical vapor deposition (LPMOCVD) [6], mechano-synthesis [7], selenization technique [8], mechanical alloying [9]. FeSe thin films with the preferred electrical and optical properties are obligatory for photo electro chemical solar cells applications. It is complicated to achieve uninterrupted and lone phase FeSe thin films by the above declared techniques. Among many deposition methods, electron beam deposition is one of the appropriate methods to set up continuous and thin semiconductor films.

Current innovation of high transition temperature (T_c) superconductivity in iron foundation quaternary layered compounds has strained substantial contemplation. Narrowly trailed by the first account of superconductivity with Curie Temperature $T_c=26^\circ\text{K}$ in $\text{LaFeAsO}_{1-x}\text{F}_x$ [10], more than a few analogous but simpler ternary and binary layered compounds, $\text{Ba}_{1-x}\text{K}_x\text{FeAs}_2$ (122-family) [5], LiFeAs (111-family) [6], and FeSe (11-family), were originate superconductivity that might have the same origin as the 1111 plane relations.

In II-VI semiconductors, considerable attention has been devoted to the possibility of tailoring the optical and electrical properties of these materials. This purpose has been mainly achieved by means of two different processes: (i) the doping with different dopant density, which

***Corresponding author:** Ayeshamariam A, Research and Development Center, Bharathiyar University, Coimbatore, 641046, India, Tel: +91 +4565-241539; E-mail: aismma786@gmail.com

Chandra Mohan R, Department of Physics, Sree Sevugan Annamalai College, Devakottai, 630303, India, E-mail: rathinam.chandramohan@gmail.com

Received March 10, 2017; Accepted April 18, 2017; Published April 28, 2017

Citation: Segu Sahuban Bathusha NM, Chandra Mohan R, Saravana Kumar. S, Ayeshamariam A, Jayachandran M (2017) Micro Structural and Optical Properties of Ferrous Selenide Thin Films and Its Characterization. Fluid Mech Open Acc 4: 156. doi: [10.4172/2476-2296.1000156](https://doi.org/10.4172/2476-2296.1000156)

Copyright: © 2017 Segu Sahuban Bathusha NM, et al. This is an open-access article distributed under the terms of the Creative Commons Attribution License, which permits unrestricted use, distribution, and reproduction in any medium, provided the original author and source are credited.

causes the broadening of band tails and band gap renormalization. (ii) The fabrication of ternary and quaternary alloys, whose band gap can be modulated by controlling the relative concentration of two elements forming the alloy. It is a well known fact that the quality of the devices based on CdSe thin films strongly depends on the structural and electrical properties of the films obtained under various experimental conditions. [6-10]. A comparison of made known data designates that large number of literature is available regarding ferrous disulfide (FeS_2) thin films, but a hardly quite a few reports are available on FeSe thin films. The original compounds those undoped of the 1111 and 122 families experience a phase transition and structural distortion at low temperature (T_s) followed by an antiferromagnetic (AFM) status developed at equal or rather lower temperatures, where the high superconductivity materializes only when this magnetic state was suppressed together with the phase transition by doping or applying pressure externally [9-12].

On the other hand, Mossbauer and Selenide Nuclear Magnetic Resonance (NMR) measurements recommended that AFM spin fluctuations are strappingly superior near T_c [3,10]. By means of spin rotation method, it was confirmed that a static magnetic order might emerge above at applied pressure non transiting the 122-family [13-15], high-quality mono crystals of 1111 family and FeSe are small are usually plate-like measuring a few hundreds of micrometer across and tens of micrometer thick [16-18]. In this esteem, the preparation of high quality thin film samples not only satisfies the requirements for some fundamental physical properties measurements other than also provides appropriate bases for making tunneling junctions that resolves more than a few imperative superconducting parameters such as gap value and paring equilibrium. Additionally the epitaxial thin films are also apposite for studying the uniaxial pressure dependence of superconducting properties by introducing interfacial stress between thin films and the substrates base. Lately it was showed that the strain induced by the film and substrate interface suppresses the low temperature phase transition in conjunction with the superconductivity for FeSe thin film within definite desired orientations [14]. Meanwhile, it was also told that superconducting Thin films of $\text{Sr}(\text{Fe}_{1-x}\text{Co}_x)_2\text{As}_2$ and $\text{Ba}(\text{Fe}_{1-x}\text{Co}_x)_2\text{As}_2$, correspondingly, while thin films of FeSe, Ferrous Telenide (FeTe) and $\text{FeSe}_{1-x}\text{Te}_x$ were as well revealed to have superconductivity. In recent times, The first superconducting epitaxial $\text{LaFeAsO}_{1-x}\text{F}_x$ thin film with analogous T_c to that of bulk, by growing at room temperature followed with 7h post annealing at 960°C in vacuum [17-19].

The interfaces and surfaces have significant functions in nanostructured materials as they have very specific surface areas for reactions. The grain size of the nanostructured material has large number of atoms at edge and corner sites, which enlarges number of reactive vigorous sites. Numerous magnetic materials together with reduced magnetic semiconductors and metallic and semi metallic Ferro magnets have been grown on Gallium Arsenide (GaAs) substrates very frequently.

Ferrous Selenide (FeSe), since a magnetic material with Curie temperature greater than room temperature, besides might be grown on GaAs and Silicon (Si) substrates. In earlier studies, highly familiarized single phase FeSe thin films were fabricated by metal organic chemical vapor deposition and the electronic and magnetic properties have been researched [13-15]. The measurement made by Hall designated that as grown FeSe thin film with hole concentration of as high as 10^{20} - 10^{21} cm^{-3} and was p-type conduction. It was seen that the critical behavior in the temperature-dependent resistivity characteristics has been observed

around 290 K for $\text{Fe}_{0.48}\text{Se}_{0.52}$ and also establish that the properties of FeSe films are sensitive to the growth conditions. On the other hand, the relationship between electronic and magnetic properties of FeSe films is not understandable. For the time being, minute information about the magnetic an isotropy which is one of the important parameter for the application of spintronic devices that can be scrutinized. It is found that the structural, electrical, and magnetic properties of FeSe film fabricated by low pressure metal organic chemical vapor deposition are ferromagnetic with the Curie temperature T_c around 305 K. A four probe method with annealed indium pads as ohmic contacts is used to measure the temperature dependent resistivity.

The preferred growth of thin films along the c -axis shows a brawny thickness dependent suppression of superconductivity and low temperature structural deformation. Quite the reverse, mutual properties are less affected in the films with preferred orientation in (101) plane. These consequences propose that the low temperature structural distortion is closely associated with the superconductivity of the material of FeSe films. The detection of Fe based superconductors has motivated worldwide attention both experimentally and theoretically. The ordinary characteristic of all the F based superconductor compounds is that they have Fe_x layers ($X=\text{P, As, S, Se, Te}$) compiled of edge to edge sharing tetra and hexa with an Fe at the center.

The superconducting combination is considered to happen in the FeX layers and it can be persuaded both by hole or electron doping through chemical substitution or by high pressure. It was extensively believed that in Fe-based superconductors, the As via anti ferromagnetic super exchange interaction between the next nearest neighbouring Fe-Fe atoms participates an important function. This sort of interface depends strappingly on the limited geometry of an Fe-As bond. Undeniably, it was initiated that the geometry of the Fe tetrahedral unit, in fastidious, the bond length and the bond angle strongly correlates with the superconductivity transition temperature between two neighbouring X and Fe ions. It was found that in contracts to from the metallic bulk FeSe, mutually monolayer and bilayer thin films demonstrated a semiconducting behaviour with a collinear AFM order on Fe atoms. In view of the dissimilarity between the mono layer FeSe and multilayer FeSe thin films, it can be proposed that the examined superconductivity occurs either at the interface of FeSe- SrTiO_3 or just in the first FeSe layer, but not in the other FeSe layers.

The parameters such as crystallite size, strain, dislocation density are calculated from X-ray diffraction studies. Optical absorption measurements were used to estimate the band gap value of iron selenide thin films deposited at various bath temperatures. Scanning electron microscopy (SEM) was used to study the surface morphology. The composition of FeSe thin films was analyzed using an energy dispersive analysis by Xrays (EDX) set up attached with scanning electron microscopy. Preliminary studies for photo electrochemical solar cells based on iron selenide thin films were carried out and the experimental observations are discussed [20-22].

In the present case the film surfaces were analyzed by Nano scope-III atomic force microscope with STM attachment. The AFM studies also offers the information regarding surface homogeneity, uniformity, nanostructure, nature of grains and other special features of the films, that are in nano meter regim. Also AFM is the basic confirmation tool and plays an important role in nano technology, which deals with the rearrangement/architecture of atoms so as to perform our desired function in the nano meter scale.

Ubale et al reported that, the 2D and 3D AFM image of FeSe film

confirms uniform deposition with porous morphology. The EDAX study reveals that their on selenide films are rich in iron. The absorption spectrum indicates that the spray deposited FeSe films have direct transition with optical band gap 2.75eV. The electrical resistivity at room temperature is of the order of 10^3 - 10^4 ohm-cm and its variation with temperature reconfirms semi conducting behavior of FeSe [23].

Maryam et al reported that, Silver selenide (Ag_2Se) nanoparticles have been sonochemically synthesized from the reaction of AgNO_3 and SeCl_4 as precursors, in the presence of thiourea ($\text{CH}_4\text{N}_2\text{S}$) and hydrazine hydrate ($\text{N}_2\text{H}_4 \cdot \text{H}_2\text{O}$). It is found that the ultrasonic power, reaction time and temperature and molar ratio between AgNO_3 and SeCl_4 play important roles in controlling the composition and particle size of products [9,24-26].

Satoshi Demura et al reported that, FeSe films were synthesised by the electrochemical deposition in the electrolyte containing $\text{FeCl}_2 \cdot 4\text{H}_2\text{O}$, SeO_2 and Na_2SO_4 . The composition ratio of Fe and Se was controlled by the synthesis voltage and pH value. The FeSe film with the composition ratio of Fe:Se 1:1 is fabricated at a voltage of 0.9 V and pH 2.1 in electro chemical deposition [27].

Experimental Section

Thin films of FeSe were prepared by electron beam evaporation (EB) technique using a HINDHI-VAC vacuum unit (model: 12A4D) fitted with electron beam power supply (model: EBG-PS-3K). For target preparation, 500 mg of spectroscopically pure Ferric nitrate (99.99%) was mixed with 2.5 mg of Selenium di oxide (SeO_2) using a pestle and mortar. The mixture was pressed into pellets by hydraulic method to get pellet with a pressure of 500 kg/cm², which was used as the source material for evaporation. The pellet was taken in a graphite crucible and kept in water cooled copper hearth of the electron gun. The pelletized FeSe targets were heated by means of an electron beam collimated from the direct current heated tungsten filament cathode. The surface of the FeSe pellet was bombarded by 180°C deflected electron beam with an accelerating voltage of 5 KV and a power density of ~ 1.5 KW/cm².

The evaporated species from FeSe pellet were deposited as thin films on the substrates in a pressure of about 1×10^{-5} mbar. Each substrate was placed normal to the line of sight from the evaporation source at a polar angle to avoid shadow effects and also to obtain uniform deposition. The different preparation parameters such as source to substrate distance (15 cm) and partial pressure (10^{-5} mbar) have been varied and optimized for depositing uniform, well adherent and transparent films. The rate of evaporation (0.5 nm/s) was used to deposit all FeSe films. The deposited FeSe films at 0.5×10^{-2} Pa oxygen pressure were annealed at RT, 100°C, 200°C and 300°C respectively to study the effect of annealing temperature on the structural, optical, and morphological properties.

Result and Discussion

X-Ray diffraction (XRD) analysis

X-ray diffraction analysis was carried out in order to determine the crystalline nature and phases of the deposited films at various temperature ranges from RT, 100, 200 and 300°C respectively (Figure 1). Using X-ray diffraction data, the inter planar spacing d_{hkl} was calculated from the Bragg's relation:

$$d_{hkl} = \lambda / (2 \sin \theta)$$

Where

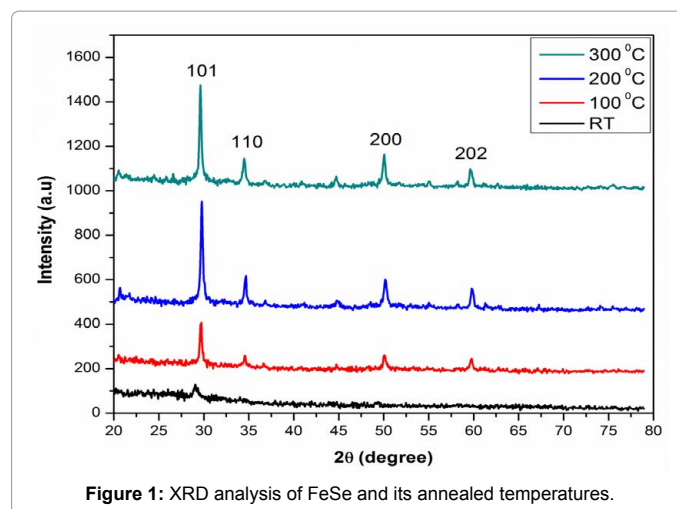


Figure 1: XRD analysis of FeSe and its annealed temperatures.

λ is the wavelength of X-rays,

d is the inter planar spacing,

n is the order number.

The factor ' d ' is related to (hkl) indices of the plane and dimension of the unit cell. From X-ray diffraction data, the crystallite size of the deposited films was calculated using Full Width at Half Maximum (FWHM) data and Debye-Scherrer formula $D = 0.9 \lambda / (\beta \cos \theta)$

Where,

λ is the wavelength of CuK α radiation ($\lambda = 1.540 \text{ \AA}$),

β is the full width at half maximum of the peak in radians

θ is Bragg's diffraction angle at peak position in degrees.

Dislocation density is defined as the length of dislocation lines per unit volume of the crystal (Williamson and Smallman) [17]. The dislocation density (δ) is given by

$$\delta = 1/D^2$$

The origin of the micro strain is related to the lattice misfit, which in turn depends upon the deposition conditions. The micro strain can be calculated from the relation,

$$\epsilon = (\beta \cos \theta) / 4$$

The c -axis lattice constant of the FeSe film can be obtained from the diffraction angle by the formula $2d \sin \theta = n\lambda$. From the experimentally measured positions of (101), (110), (200) and (202) diffraction peaks, we have calculated that the c -axis lattice constant is about 0.5498 nm, which is a little smaller than 0.5518 nm bulk FeSe. Little of Fe vacancies can be responsible for this slight decrease of perpendicular component of lattice constant. It can be seen clearly that phase peaks emerges up as with increasing the temperature. The calculated lattice parameter values (a' and c') show in very close agreement with the standard values.

It is observed from Table 1 that the crystallite size increases with annealing temperature and attained a maximum value at annealing temperature of 300°C. The rms micro strain, on the other hand decreases gradually with increase in annealing temperature and attained a minimum value for a typical FeSe film deposited at different annealing temperatures from RT to 300°C. As the annealing temperature raises, a great number of Fe and Se ions gets adsorbed on the substrate which

Temperature (°C)	Crystal size D (nm)	Dislocation density δ ($\times 10^{14}$) lines/m ²	Strain $\epsilon \times 10^{-3}$	No of crystallites $n \times 10^{15}$ /unit area	Lattice parameters		Bandgap (eV)
					a (nm)	c (nm)	
RT	21	23.7	2.12	20.7	3.705	5.51	2.85
100	28	21.8	2.06	16.2	3.699	5.495	2.81
200	44	18.7	1.91	9.5	3.697	5.497	2.79
300	47	19.2	2.01	8.96	3.626	5.499	2.75

Table 1: Strutural studies of FeSe thin films and its annealed temperatures.

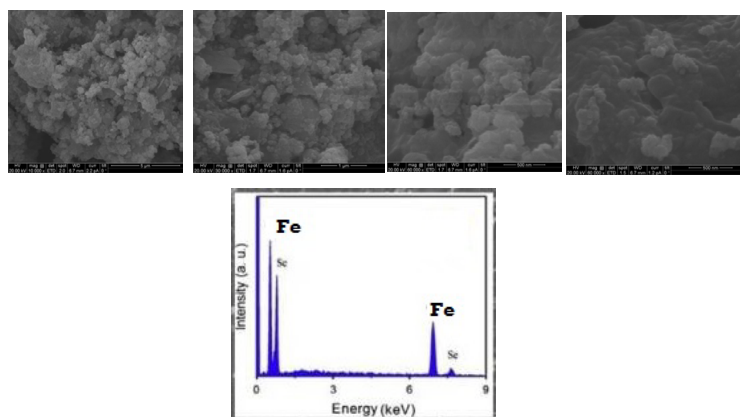


Figure 2: (a-e) SEM images of FeSe thin films annealed at different temperatures. Films annealed at different temperatures.

leads to crystallization. The crystallite size is observed to increase with film thickness and maximum value is obtained for a film of thickness of 48 nm at 300°C. Consequently, for thinner films, the micro strain and the dislocation density are found to be outsized. Throughout the strengthening of film thickness the dislocation density and micro strain are reduced due to the release of stress in the films. Moreover with the increase of film thickness, the crystallite size amplifies steadily and leans to accomplish saturation for higher thicknesses (Table 1).

At higher temperature the lattice distortion in the FeSe film is perceptibly not affected by the substrate strain effect because the film aligns preferably along (101) direction. All of these results strappingly maintain the conjecture that the dependence of opticity and conductivity on film thickness is connected with the aptitude of the lattice to undergo low temperature structural distortion, and supplementary authenticate the importance of the low temperature structural distortion to the origin of superconductivity in the FeSe scheme.

Morphological Analysis

The surface morphology of FeSe thin films was investigated by means of scanning electron microscope (SEM), elemental diffraction spectrometry (EDS), and high resolution transmission electron microscopy (TEM).

The SEM pictures of FeSe thin films annealed at different temperatures (room temperature, 100, 200 and 300°C) are shown in Figure 2a-2e. It is observed from the SEM images that the films deposited at RT have appeared to be rougher and demonstrates coarse like structure. At higher temperatures (100-300°C) the films surface is covered with uniform spherically shaped grains. The grains visible in SEM picture thus represent aggregates of very many small crystallites. The sizes of the grains are found to be in the range between 28 and 48 nm respectively. The average sizes of the grains are found to be 35 nm.

Compositional Analysis

The composition of the films was investigated using an energy

dispersive analysis by X-rays (EDX) set up attached with scanning electron microscope. The EDAX results revealed that the following composition in at percentage: For deposited film Fe is 67.30%, Se is 6.72%, for film annealed at 100°C Fe is 69.45%, Se 7.01%, for film annealed at 200°C Fe is 67.29%, Se is 6.96% and film annealed at 300°C Fe is 73.14%, Se is 6.18%.

Modern researches on the tetragonal phase FeSe (spacegroup P4/nmm) have exposed that they endure a structural phase transformation from 90 K(Ts), to orthorhombic phase (space group Cmma), concerning chiefly a insignificant distortion in(a-b) plane, i.e., γ tetragonal angle slightly enlarged from 90°, as it turns out to be superconducting at 8K (Tc) [7,10,20]. Through varying the stoichiometry of FeSe, for instance totalling extra iron [10,12], or doping with alien atoms, like substitution of iron with copper [21], the low temperature structural distortion could be suppressed along with the c-axis.

For thin-film samples, we have shown that by depositing at lower temperature, e.g. at room temperature, the a-b plane of tetragonal FeSe sits well at glass/Si substrate and the limitations to low temperature structural distortion becomes stronger as the film grown emaciated. If the films deposited at higher temperature, like 100-300°C, the film favoured orientation changes from [001] to [101] and the film/ substrate interface broadens, resulting in more thickness independent superconductivity and more sharp opticity.

AFM (Dimension 3100 controller Nanoscope IIIa, Digital Instruments, Veeco, Metrology Group) was used to characterize contact mode at ambient temperature was done to further investigate the morphology of the FeSe films. Root mean square (rms) surface roughness value was determined on an area of 10 $\mu\text{m} \times 10 \mu\text{m}$ for all samples. The roughness analyses software provided by the instrument manufacturer was used to calculated rms. Through (Figure 3a-3d) results, AFM surface morphologies of iron selenide films synthesized at diverse temperatures.

AS-deposited FeSe thin film was investigated by taking AFM images

through two and three dimensional surface morphology. Figure 3a-3d shows the 3D and 2D AFM images of FeSe films annealed at different temperatures. From the micrographs, one can see the total coverage of the substrate with uniform growth of spherical grains. The rms roughness of film surface is 6.32, 10.03, 14.46 and 30.78 nm for the films of thickness 29.7, 50.9, 69.1 and 106 nm 156 and 270 nm respectively at temperatures RT, 100°C, 200°C and 300°C. The surface for the deposited film at lower thickness is almost smooth and independent of the scanning area selected.

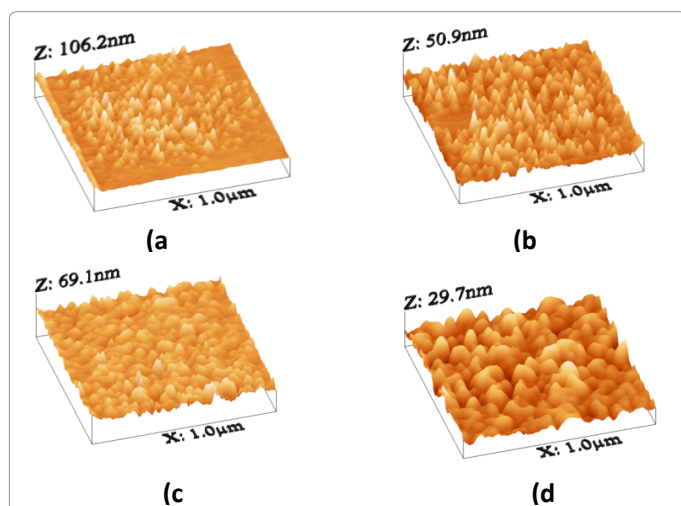


Figure 3: (a-d) 3D images of FeSe thin films annealed at different temperatures.

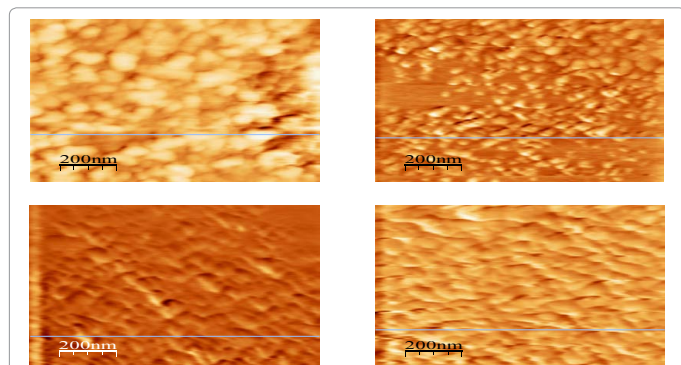


Figure 4: (a-d) 2D images of FeSe thin.

The images produced by AFM illustrate that the films are relatively porous clusters and have a rough surface (Figure 3a-3d). A clustered structure on which some grains are grown is shown in Figure 4a-4d. The AFM views of films selenized at 300°C have a quite different morphology than that of those selenized at 100°C. Asymmetrical spherical and cylindrical crystallites were observed (Figures 3a-3d) verifying the occurrence of more than one phase as observed by SEM as shown in Figure 2a-2b. A strapping roughness was observed for these layers for films produced at 300°C, when great grain size dimensions were examined in Figure 4a-4d in 2-D AFM images.

Optical Transmittance Behavior with Temperature

Study of FeSe thin films by recording the transmission spectra gives information about the optical features of semiconductor films about their band structure and its influence on the variation of deposition temperatures. Mainly grain size changes show observable influence in the present study.

The transmission spectra of the films deposited at different substrate temperatures was studied in the wavelength range 450 to 2500 nm.

$$A\hbar\nu = A(\hbar\nu - E_g)^{1/2}$$

Figure 3 shows the transmission spectra of the FeSe films deposited at as deposited, 100, 200 and 300°C respectively.

The spectra exhibit interference fringes. The absorption co-efficient (α) was estimated from the transmission spectra. In order to find out the nature of the band gap of the FeSe films, i.e. direct or in-direct band gap, α and $\hbar\nu$ values were used to fit-in with the above equation,

For direct band gap, where E_g is the band gap of the FeSe films, α is the absorption coefficient, A is the constant and $\hbar\nu$ is the photon energy. The $(\alpha\hbar\nu)^2$ versus $(\hbar\nu)$ plots (Figure 5a-5b), for all the films deposited on glass substrates, show straight line portions which cut the $\hbar\nu$ axis (x-axis) on extrapolation giving the band gap values. It is observed that all graphs for the films deposited at different substrate temperatures have straight line portions in the high energy region which confirms the direct band gap nature for all the FeSe films prepared by EB evaporation technique. The value of E_g values are 2.87, 2.85, 2.82 and 2.78 eV for the FeSe films deposited on glass substrates at RT, 100, 200 and 300°C respectively. It is observed that the E_g value decreases with increasing substrate temperature. Which, in turn, depend on the increase of grain/particle size of the FeSe films with increasing substrate temperature, such observations have been reported for spray pyrolysis deposited films [22,23].

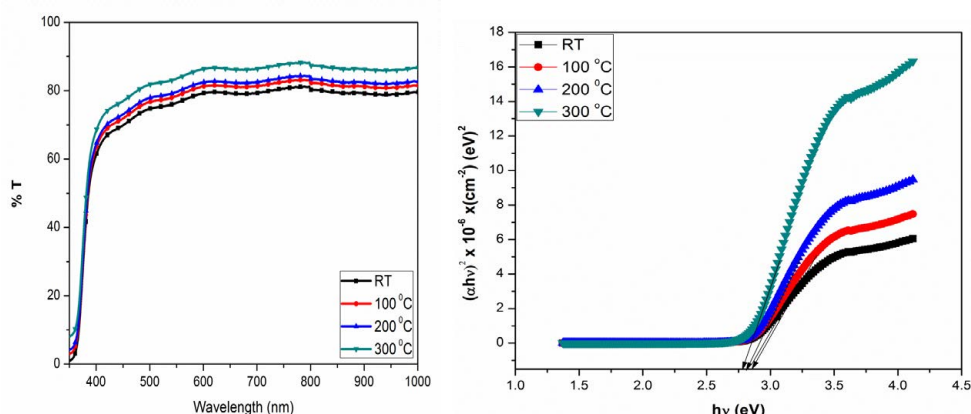


Figure 5: (a and b) UV-Vis Transmittance spectra and plot of $(\alpha\hbar\nu)^2$ vs. $\hbar\nu$ for as deposited and annealed FeSe thin films.

The intersection point gives the direct band gap of the material and is found to be 1.24 eV. It is established that the band gap value of the samples obtained in this work is slightly higher than the value reported earlier for electrodeposited FeSe.

Conclusion

The FeSe thin films were deposited using Electron beam deposition method on Si substrates by changing molar concentration of $\text{Fe}(\text{NO}_3)_3 \cdot 9\text{H}_2\text{O}$ 0.03 from to 0.18 M. The XRD study for FeSe thin film deposited showed tetragonal crystal structure. The SEM and AFM studies show cluster of porous morphology. The optical studies were calculated by AFM and UV-vis spectroscopy. The results revealed that thickness and roughness of surface is directly related to the temperate changes that were varied during the film deposition.

References

- Mahalingam T, John VS, Rajendran S, Sebastian PJ (2002) Electrochemical deposition of ZnTe thin films. *Semicond Sci Technol* 17: 465-470.
- Julie DM, Michael C (1996) Properties of Zinc Telluride Containing Impurities Introduced during Spray Pyrolysis. *J Electrochem Soc* 143: 4054-4059.
- Rotter M, Tegel M, Johrendt D (2008) Superconductivity at 38 K in the Iron Arsenide $(\text{Ba}_{1-x}\text{K}_x)\text{Fe}_2\text{As}_2$. *Phys Rev Lett* 101: 107006.
- Kamimura T, Kamigaki K, Hirose T, Sato K (1967) On the Magnetocrystalline Anisotropy of Iron Selenide Fe_7Se_8 . *J Phys Soc Jpn* 22: 1235.
- Hamdadou N, Khelil A, Bernede JC (2003) Bernede. *Mater Chem Phys* 78: 591-601.
- Wu XJ, Zhang ZZ, Zhang JY, Ju ZG, Shen DZ, Li BH, et al. *J Cryst Growth* 2007300: 483-485.
- Campos CEM, de Lima JC, Grandi TA, Machado KD, Itie JP, Polian A (2004) Pressure-induced effects on the structural properties of iron selenides produced by mechano-synthesis. *J Phys Condens Matter* 16: 8485-8490.
- Hamdadou N, Bernede JC, Khelil A (2002) Preparation of Iron Selenide Films by Selenization Technique. *J Cryst Growth* 241: 313-319.
- Campos CEM, de Lima JC, Grandi TA, Machado KD, Pizani PS (2002) *Solid State Commun* 123: 179-184.
- Kamihara Y, Hiramatsu H, Hirano M, Kawamura R, Yanagi H, et al. (2006) Iron-Based Layered Superconductor: LaOFeP . *J Am Chem Soc* 128: 10012-10013.
- Takahashi H, Igawa K, Arii K, Kamihara Y, Hirano M, et al. (2008) Superconductivity at 43 K in an iron-based layered compound $\text{LaO}_{1-x}\text{F}_x\text{FeAs}$. *Nature* 453: 376.
- Kamihara Y, Watanabe T, Hirano M, Hosono H (2008) Iron-Based Layered Superconductor $\text{La}[\text{O}_{1-x}\text{F}_x]\text{FeAs}$ ($x=0.05-0.12$) with $T_c=26$ K. *Chem Soc* 130: 3296-3297.
- Hsu FC, Luo JY, Yeh KW, Chen TK, Huang TW, et al. (2008) Superconductivity in the PbO-type structure $\alpha\text{-FeSe}$. *Proc Natl Acad Sci* 105: 14262.
- de la Cruz C, Huang Q, Lynn JW, Li JY, Ratcliff W (2008) Magnetic order close to superconductivity in the iron-based layered $\text{LaO}_{1-x}\text{F}_x\text{FeAs}$ systems. *Nature* 453: 899.
- Kimber SAJ, Kreyssig A, Zhang YZ, Jeschke HO, Valenti R, et al. (2009) Similarities between structural distortions under pressure and chemical doping in superconducting BaFe_2As_2 . *Nat Mater* 8: 471.
- McQueen TM, Williams AJ, Stephens PW, Tao J, Zhu Y, et al. (2009) Tetragonal-to-Orthorhombic Structural Phase Transition at 90 K in the Superconductor $\text{Fe}_{1.01}\text{Se}$. *Phys Rev Lett* 103: 057002.
- Hiramatsu H, Katase T, Kamiya T, Hirano M, Hosono H (2008) Superconductivity in Epitaxial Thin Films of Co-Doped SrFe_2As_2 with Bilayered FeAs Structures and their Magnetic Anisotropy. *Appl Phys Express* 1: 101702.
- Iida K, Hanisch J, Hühne R, Kurth F, Kizun M, et al. (2009) Strong T_c dependence for strained epitaxial $\text{Ba}(\text{Fe}_{1-x}\text{Co}_x)_2\text{As}_2$. *Appl Phys Lett* 95: 192501.
- Han Y, Li WY, Cao LX, Zhang S, Xu B, et al. (2009) Preparation and superconductivity of iron selenide thin films. *J Phys C* 21: 235702.
- Han Y, Li WY, Cao LX, Wang XY, Xu B, Zhao BR, et al. (2010) Superconductivity in Iron Telluride Thin Films under Tensile Stress. *Phys Rev Lett* 104: 017003.
- Takemura Y, Suto H, Honda N, Kakuno K (1997) Characterization of FeSe thin films prepared on GaAs substrate by selenization technique. *J Appl Phys* 81: 5177.
- Maryam J, Sobhani A, Salavati-Niasari M (2014) *Journal of Industrial and Engineering Chemistry* 20.5 (2014)3775-3779.
- Ubale AU, Sakhare YS, Belkedkar MR, Singh A (2013) Characterization of nanostructured iron selenide thin films grown by chemical route at room temperature. *Materials Research Bulletin* 48: 863-868.
- Sydlik SA, Lee JH, Walish JJ, Thomas EL, Swager TM (2013) Epoxy functionalized multi-walled carbon nanotubes for improved adhesives. *Carbon* 59: 109-120.
- Das S, Lahiri D, Lee DY, Agarwal A, Choi W (2013) Measurements of the adhesion energy of graphene to metallic Substrates. *Carbon* 59: 121-129.
- Hamdadou N, Bernede JC, Khelil A (2002) *J Cryst Growth* 241: 313.
- Ouertani B, Ouertelli J, Saadoun M, Bessai B, Hajji M, et al. (2005) *Mater Lett* 59 (2005) 734.